

The diamond (111) surface reconstruction and epitaxial graphene interface

Benjamin P. Reed,^{a,b,c} Marianne E. Bathen,^d Jonathan W. R. Ash,^{a,b} Claire J. Meara,^{b,e} Alexei A. Zakharov,^f Jonathan P. Goss,^e Justin W. Wells,^g D. Andrew Evans^a and Simon P. Cool^{a,g}

^a Department of Physics, Aberystwyth University, Aberystwyth, SY23 3BZ, United Kingdom.

^b Centre for Doctoral Training in Diamond Science and Technology, University of Warwick, Coventry, CV4 7AL, United Kingdom.

^c National Physical Laboratory, Teddington, TW11 0LW, United Kingdom.

^d Advanced Power Semiconductor Laboratory, ETH Zurich, Zurich, 8092, Switzerland.

^e School of Electrical and Electronic Engineering, Newcastle University, Newcastle-upon-Tyne, NE1 7RU, United Kingdom.

^f Max IV Laboratory, Lund University, Lund, 221 00, Sweden.

^g Centre for Materials Science and Nanotechnology, University of Oslo, Oslo, 0318, Norway.

Supplemental materials from *Phys. Rev. B* 105, 205304 (2022).

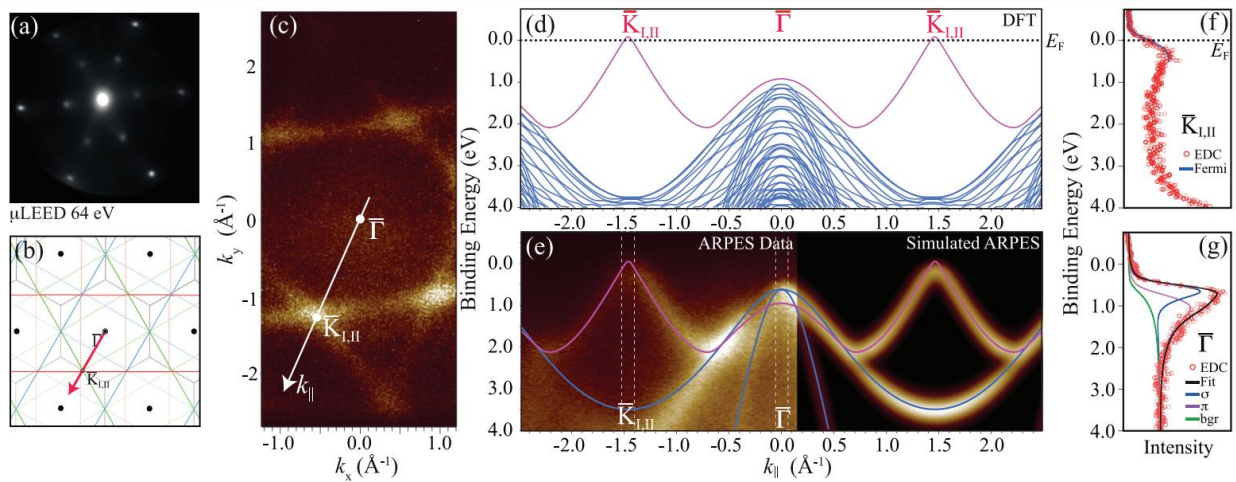


Figure 1. μ LEED, ARPES, and DFT results from the C(111)-(2 \times 1) surface reconstruction following in vacuo annealing at 920°C. (a) μ LEED pattern acquired at a kinetic energy of 64 eV; spots from all three rotational domains are observed with comparable intensity. (b) Schematic diagram of the Γ - $K_{1,II}$ direction through the surface Brillouin Zones used for the DFT and ARPES data sets presented in panels (d) and (e), respectively. (c) Constant energy surface from the ARPES data set at $E_B = 0.1$ eV. The white arrow indicates the direction of the slice used to produce the E vs $k_{||}$ data shown in (e). (d) DFT results of the occupied valence band structure; the π -band originating from the reconstruction is shown in magenta and the bulk σ bands in blue. (e) Photoemission intensity on the left-hand side and the simulated intensity on the right. Overlaid on the image is the π -band that results from the 64-atom DFT supercell calculation in magenta, along with the bulk σ bands from the simple 2-atom unit cell DFT calculation in blue. The white vertical lines are the boundaries of the integrated area used for the EDCs at $K_{1,II}$ and Γ shown in panels (f) and (g), respectively. [Reproduced from *Phys. Rev. B* 105, 205304 (2022), which is the authors' own work]

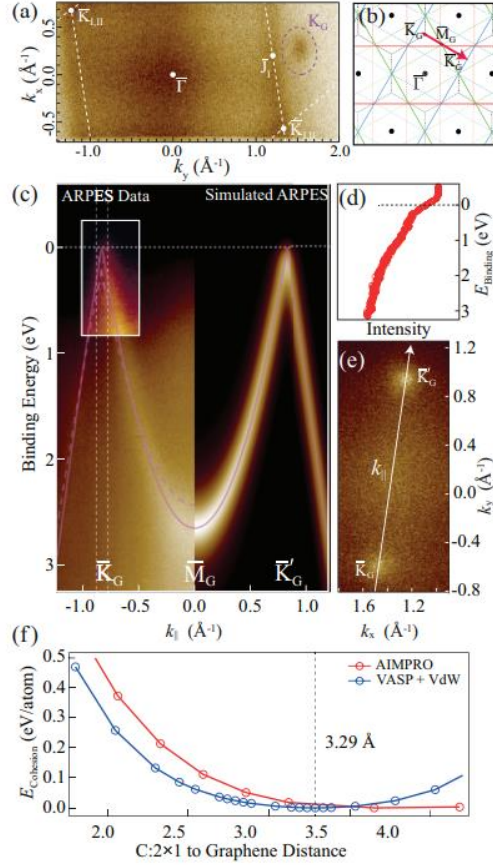


Figure 2. ARPES measurements and DFT calculations of graphene formed above the C:2 \times 1(111) surface. (a) Constant energy surface at $E_B = 0.1$ eV using $h\nu = 125$ eV. The graphene K_G point is circled in a magenta dotted line, and the white dotted lines are to guide the eye toward the hexagram features already discussed for the C(111)-(2 \times 1) surface. (b) Schematic diagram showing the K_G - M_G - K_G '- Γ ' direction along the edge of graphene's hexagonal BZ. (c) Photoemission intensity, DFT-calculated bare bands, and simulated intensity. The ARPES data set on the left-hand side was acquired with $h\nu = 40.8$ eV. Overlaid on the image are the DFT-calculated π -band as the dashed magenta line, and the same band after performing a rigid shift and stretch as a solid magenta line. The solid line is used for creating the simulated ARPES intensity on the right. (d) EDC taken at the K_G point with a width of 0.1 \AA^{-1} integrated between the vertical dashed white lines in (c). (e) Constant energy surface at E_F , using $h\nu = 40.8$ eV; the white arrow indicates the slice taken to extract the E vs $k_{||}$ data sets shown in (c). (f) The graphene atoms' cohesion energy as a function of distance from the C(111)-(2 \times 1) surface both with and without vdW interactions. [Reproduced from *Phys. Rev. B* **105**, 205304 (2022), which is the authors' own work]